LEGIBILITY NOTICE

A major purpose of the Technical Information Center is to provide the broadest dissemination possible of information contained in DOE's Research and Development Reports to business, industry, the academic community, and federal, state and local governments.

Although a small portion of this report is not reproducible, it is being made available to expedite the availability of information on the research discussed herein.

LA-UR -83-1314

Conf-830580--1

MASTER

DISCLAIMER

LA-UR--83-1314

DE83 012685

TITLE: RADIATION-INDUCED TRANSIENT ATTENUATION OF PCS FIBER

AUTHOR(S): Peter B. Lyons, P-14
Larry D. Looney, P-14
James W. Ogle, P-14

SUBMITTED TO: PHOTON '83
International Conference-Exhibition on Optical Fibres
and Their Appliances
Paris, France

May 16-19, 1983

Los Alamos Los Alamos National Laboratory
Los Alamos, New Mexico 87545

FORM NO 836 R4
ST NO 2629 5/81

Radiation induced transient attenuation of PCS fiber*

P. B. Lyons, and L. D. Looney

Los Alamos National Laboratory, P.O. Box 1663, MS D40, Los Alamos, NM 87545 USA

Some applications of optical fibers require their exposure to intense radiation fields. This exposure can potentially degrade performance of a fiber data link. Research at Los Alamos National Laboratory has recently concentrated on development of an understanding of such radiation effects at short times, less than 100 ns.

In previous papers we have identified a particular type of fiber, ITT plastic-clad-silica (PCS) with Suprasil core as optimum for short time radiation-induced attenuation, but that work used very large doses of ionizing radiation, close to 1 Mrad.[1,2] For these high dose exposures, moderate success in understanding the transient nature of the attenuation was realized with a geminate recombination model.

In this paper, we report further studies with ITT PCS fiber over a range of doses and wavelengths. Data on other PCS fibers is included that provide performance comparable to the ITT product. Comparison to several fluorsilicate fibers is also included.

Experimental Method

A Febetron 706 is used to provide a 1.5 ns electron pulse that irradiates a small coil of the fiber under test. The electron beam is scattered by a thin Al foil at the exit of the Febetron to provide a more uniform deposition over the coil area. The fiber coil (length 10-50 cm) encircles a collimating aperture, behind which is a fast Faraday cup. The electron pulse is measured on every Febetron pulse as a measure of electron dose.

A tunable dye laser with an optical parametric oscillator (Chromatix CMX-4 system) provides an intense source of light with wavelength adjustable between 500 and 2000 nm. The laser and Febetron are synchronized in time such that the Febetron pulse occurs during the laser output. Biplanar vacuum diodes (ITT F4014 or FW114A) detect the light signal before and after the dosed region. Data were acquired at 600, 800 and 850nm in these measurements. The first signal is derived either from scattered light out of a coil in the input fiber or

by insertion of a bidirectional coupler into the input fiber. Both signals are recorded on Tektronix 7104 and 7844 oscilloscopes. The system is shown schematically in Figs. 1 and 2. We note in passing that apparently different attenuation recovery shapes have been seen with different detectors, particularly when PIN detectors detect the throughput signal. This has not been investigated in detail yet, but probably reflects different recovery properties of the different detectors. If any residual signal (after pulse) exists after termination of a long optical input pulse, a detector will distort the observations. Photomultipliers are notorious for after-pulsing phenomena due to ion feedback. The biplanar detectors we have identified for use here have been studied with long optical pulses and no residual pulse has been observed.

The optical parametric oscillator (OPO) is used for data beyond 600 nm. When the OPO is used, the dye laser is tuned to 600 nm. At the output of the OPO, both the shifted wavelength and the 600 nm pump wavelength are present. In normal operation, a glass filter is used at the output of the OPO to suppress the 600 nm light. For some measurements herein, that filter was removed so that both wavelengths propogated in the fiber. Additional filters are always present at the diode face and restrict the detected signals to only the OPO output wavelength. Removal of the OPO filter allowed us to test for photobleaching by 600 nm light in our measurements at 800 ns, optical power in the fiber was 5-20 watts.

Relative dosimetry is provided by the Faraday cup. This cup output is normalized to absorbed dose by comparison to radiachromic film (Far West Technology, Inc., Goleta, GA). This film provides a low mass (~ 5 mg/cm^2) monitor of absorbed dose. Calibration of the film with a ^{60}Co source confirmed the vendor's sensitivity data. The low electron energy (maximum 600 keV) of the Febetron 706 leads to concern over non-uniform dose within the fiber. This was tested by preparing a multilayer stack of the thin radiachromic films and thin Al foils. This stack was then exposed to multiple Febetron shots while the Faraday cup was recorded. The resulting data set, Fig. 3, established the conversion from observed current to dose. The mass range of the fiber cores for several of the tested fibers is shown in Fig. 3 and indicates a reasonably uniform dose through the fiber.

The conversion factor from Faraday cup signal to fiber dose was chosen to approximately model the dose over the core of the tested fiber. The use of the Faraday cup signal removes most of the large uncertainty in pulse-to-pulse stability of a Febetron. (Depending on the condition of the field-emission tube, this stability can be worse than a factor of 3.) With

the Faraday cup normalization, attenuation data repeats to about ± 20%. Since both Faraday cup output and fiber peak attenuation can be read to higher accuracy (± 10%), the remaining scatter is probably due to residual non-uniformity in the electron dose across the fiber exposure plane. For a given fiber type, the relative doses are accurate to about 10%, since multiple shots (on new fiber) are used for each data point. Absolute doses depend on the accuracy of the conversion factor from Faraday charge to dose and the film calibration and may reach 30%. Relative comparisons between two fiber types reflect only the uncertainty of the conversion factor for different core and buffer thicknesses and may reach 20%.

Experimental Data and Disucssion

ITT PCS Fiber

Data were acquired at 600, 800, and 850 nm wavelengths. Figures 4 and 5 show data at the two extreme wavelengths. Each curve is averaged over multiple shots, each shot is usually on fresh fiber. Fiber is never used for more than two shots. (The 700 kRad data are from earlier work.) Qualitatively, the curves are of similar shape, but quantitatively, the shapes are not identical. This may be graphically seen in Fig. 6 where we compare the ratio of peak attenuation to the attenuation 60 ns after the electron pulse for all three wavelengths. Since substantial recovery has occurred in this time, the 60 ns value is subject to much larger uncertainty than the peak attenuation, but a trend is evident. The highest dose values show much more rapid recovery and the longer wavelengths recover faster. However, the 700 kRad data was taken in a different geometry, cf. ref. 2, with a different field emission tube in the accelerator. The electron pulse was faster (~ 1.1 ns) for that tube and may have contributed to a higher observed "peak" value. The previous work also incorporated a high bandwidth fiber to transmit the light from the Febetron cell to the photodetectors. This introduced another splice and added complexity. Peak values for ITT T303 PCS were decreased by ~ 10% due to the bandwidth limit for hte 10 m of slow step index fiber used here. The electronics and detectors were the same type for all the data and the electronics responses were carefully tested in both measurement series. For 800 nm data, we have used the present geometry for doses up to 300-400 kRad where the ratio value is ~ 5.5 ± 0.3, unchanged from the lower doses. The 700 kRad data are presented here to emphasize that any "peak" attenuation data is strongly dependent on the time duration of the electron pulse. All of the subsequent comparisons in this paper use the standard geometry of Figs. 1 and 2 and a single field emission tube.

The peak attenuation, per kRad, is shown in Fig. 7 for the three wavelengths. Data for individual (not average) shots are shown from which data scatter can be seen as < 20% for individual shots. On a per kRad basis, substantially more damage occurs at low dose. Note that the observed peak values reflect the time dependence of the incident dose and will change for different dose rates. The relative comparison here should be valid since we do not alter the pulse shape conditions.

These data indicate a substantial increase in peak damage per kRad, different for different wavelengths, at low dose. Several hypotheses could explain this phenomenon. The curves of Fig. 7 suggest that two classes of damage sites may exist, one set of "soft" sites that damage very readily (perhaps pre-existing defects) that become saturated at moderate doses and a second class of defects created in proportion to the dose. Less pure fibers might show more of the soft sites, and to some extent this is seen in some of the all-glass data presented subsequently in this paper. The ions responsible for the early absorption may have a variety of absorption levels, differing significantly with wavelength. The data of Fig. 7 suggest benefits from longer wavelengths that need to be explored.

Preliminary data on optical photobleaching were obtained, but power levels were contrained by the available power from the OPO and the very low sensitivity of the detectors at 800 nm. For these tests, the transient attenuation at 800 nm was explored with and without a 600 nm pulse of 0.2-0.4 W in the fiber. The 800 nm power level was much higher, 10-25 W. No significant change in transient attenuation was observed for the short time scales of interest here. Better tests can occur in the future if detectors with improved sensitivity at 800 nm can be obtained. This would allow lower power levels at 800 nm and comparable power levels at 600 and 800 nm. Since Sigel has shown that photobleaching can occur, at long times, even with monochromatic light in the fiber, our data are not conclusive.

Other Fiber Types

Two additional types of PCS fiber as well as four types of fluorosilicate clad fiber were studied in the same geometry at 800 nm wavelength. These included two types of 200 μm core PCS fiber from Raychem: RSC-200 (2 batches) and KSC-200. According to the vendor RSC and KSC use the same Suprasil core material but the RSC fiber has additional proprietary processing steps. The four fluorosilicates include: Raychem VSC (240 μm clad, 200 μm

core, NA = 0.2 from manufacturer's data) and three Quartz Products QSF fluorosilicates (200 μm clad, 133 μm core, NA = 0.25 from manufacturer's data) with different OH^- concentrations 30 ppm (SD), 200 ppm (STD), and 1300 ppm (SW).

In Fig. 8 we compare the peak attenuation per kRad for all these fibers to the ITT PCS. Within the uncertainties of 20% in dose the three PCS fibers are almost identical. The data for the all-glass VSC fiber is also in agreement with ITT PCS. These five fibers, ITT T303 and the four Raychem fibers, are compared in Fig. 9 for doses near 70 kRad. In Fig. 9, only average run data are shown and the peak attenuations are normalized. In this comparison the Raychem RSC fibers do not recover quite as rapidly as the Raychem KSC, Raychem VSC, and ITT PCS fibers, the difference is only slightly outside our uncertainties, but appears to be real.

As one comparison of recovery of attenuation, we plot in Fig. 10 the ratio of peak attenuation to the value at 60 ns for various doses for all the fibers at 800 nm. The data reflect averages over many runs but still do not show smooth trends. The uncertainty in the 60 ns attenuation at low dose leads to large error bars. Again, however, the KSC, VSC, and ITT fibers are best at most doses. The RSC fibers are somewhat inferior in fast recovery. Of the larger NA fluoroscilicate fibers, only the high water (SW) fiber competes with the PCS fibers. This slower recovery of the QSF fibers is illustrated in Fig. 11. These data suggest that the Raychem proprietary processing steps to enhance the RSC "hardness" may not be appropriate when very early time transient phenomena are considered.

Conclusion

For the dose ranges studied herein, 10-150 kRad, several fibers offer very competitive transient attenuation performance. One of these fibers is an all-glass composition and may offer a useful alternative to PCS fiber in many applications. The N.A. of this all-glass fiber is considerably below that of PCS and this may limit some of its possible uses. Higher N.A. all-glass fluoroscilicates offered good performance but did not equal the performance of the best fibers.

For all the fibers studied, proportionately more damage is observed at low doses. This may be due to varying degrees of pre-existing damage sites that are depleted (damaged) at higher doses. Of critical importance, however, is the observation in Figs. 4, 5, and 6 that the functional form of the transient recovery is not changed, within our uncertainties, as

dose varies. Thus even though some phenomenon, such as our postulated pre-existing "soft" sites, leads to increased damage at low dose, the recovery mechanisms do not change with dose.

References

1. DNA Conf. . .

2. SPIE Vol. 296.

TEST ARRANGEMENT

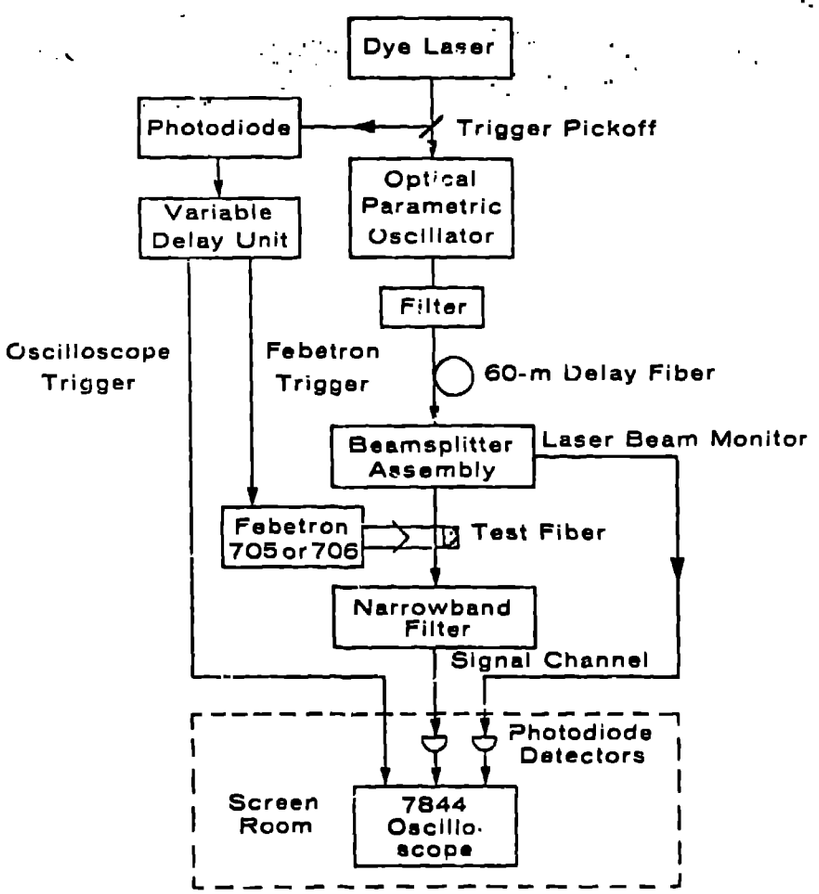

Schematic diagram of the apparatus used for transient attenuation measurements in optical fibers. The test channel recording the output of the fiber was recorded on one Tektronix 7844 in addition to the other Tektronix 7844.

LOW DOSE RADIATION ABSORPTION GEOMETRY

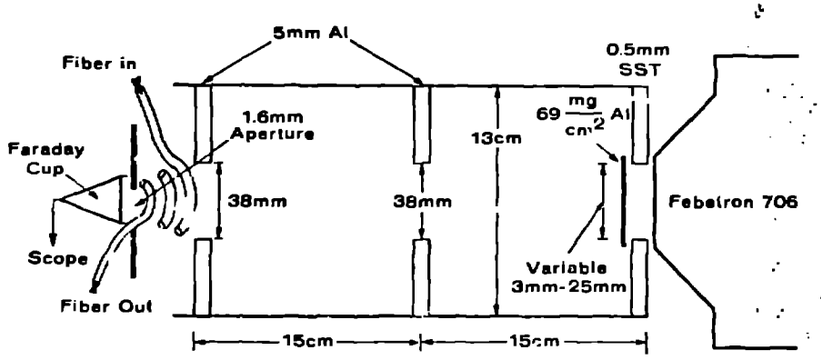

Schematic diagram of the geometry at the exit port of the Febetron 706.

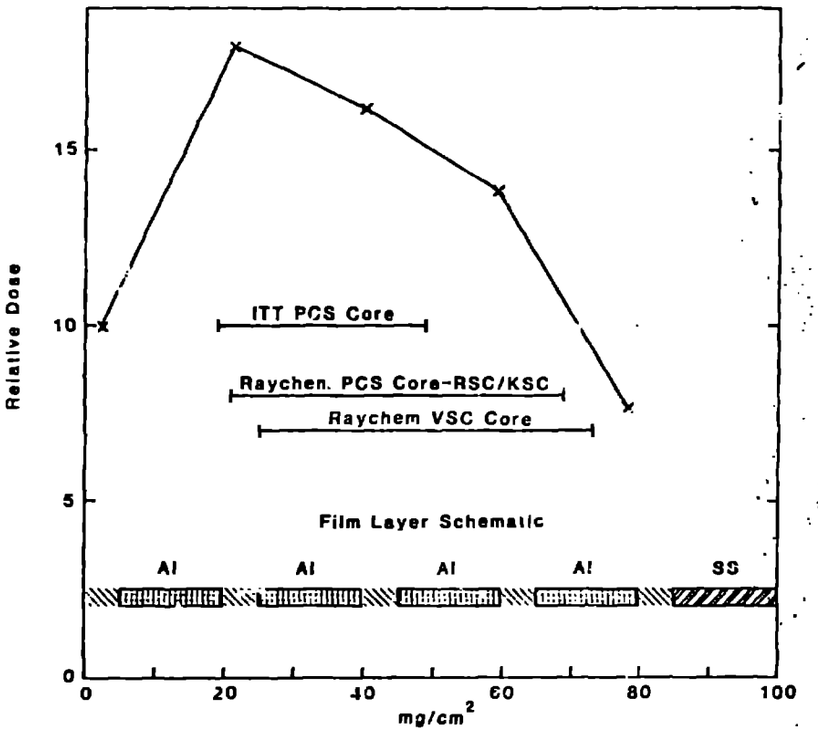
Relative Dose
15
10
5
0
ITT PCS Core
Raychen. PCS Core-RSC/KSC
Raychem VSC Core
Film Layer Schematic
Al
Al
Al
Al
SS
0
20
40
60
80
100
mg/cm²

(3)

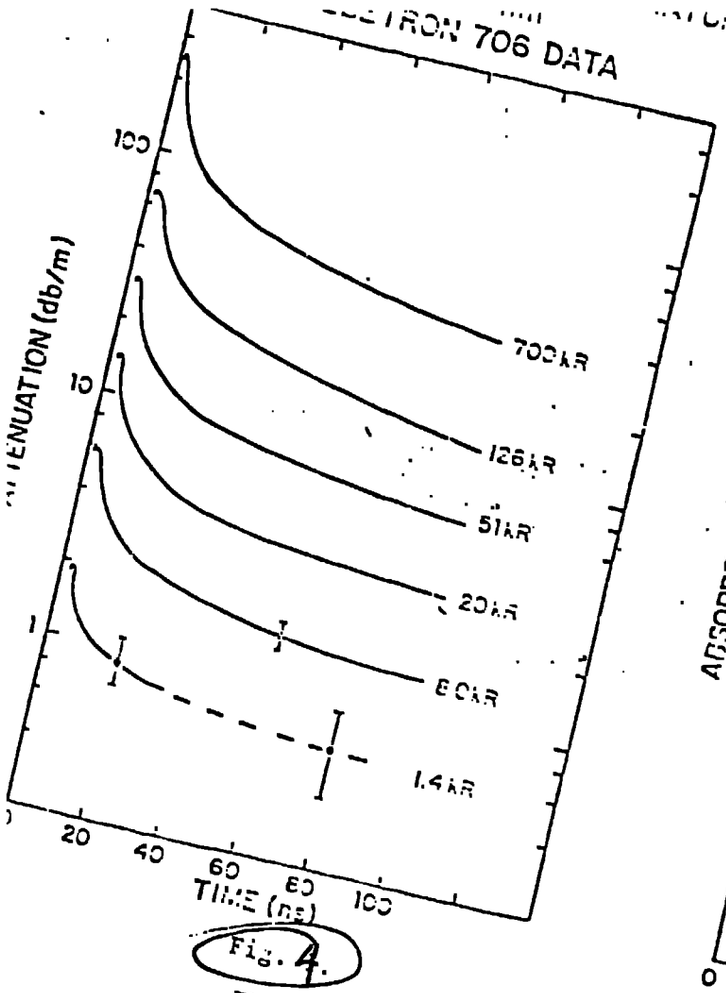

Fig. 4.

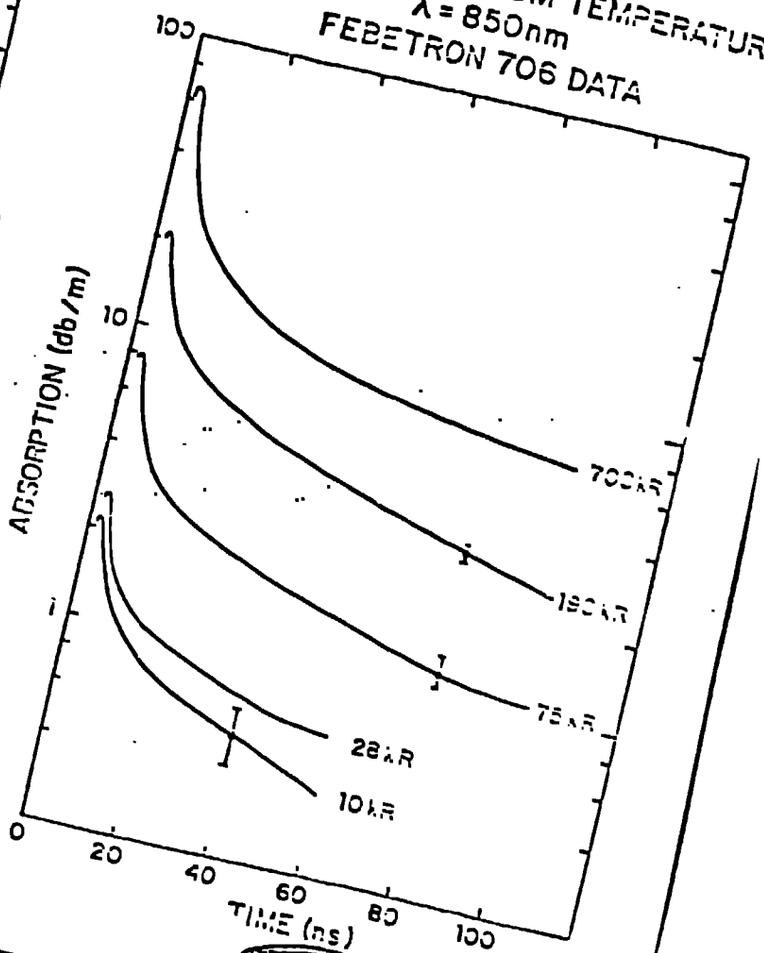

Fig. 3.

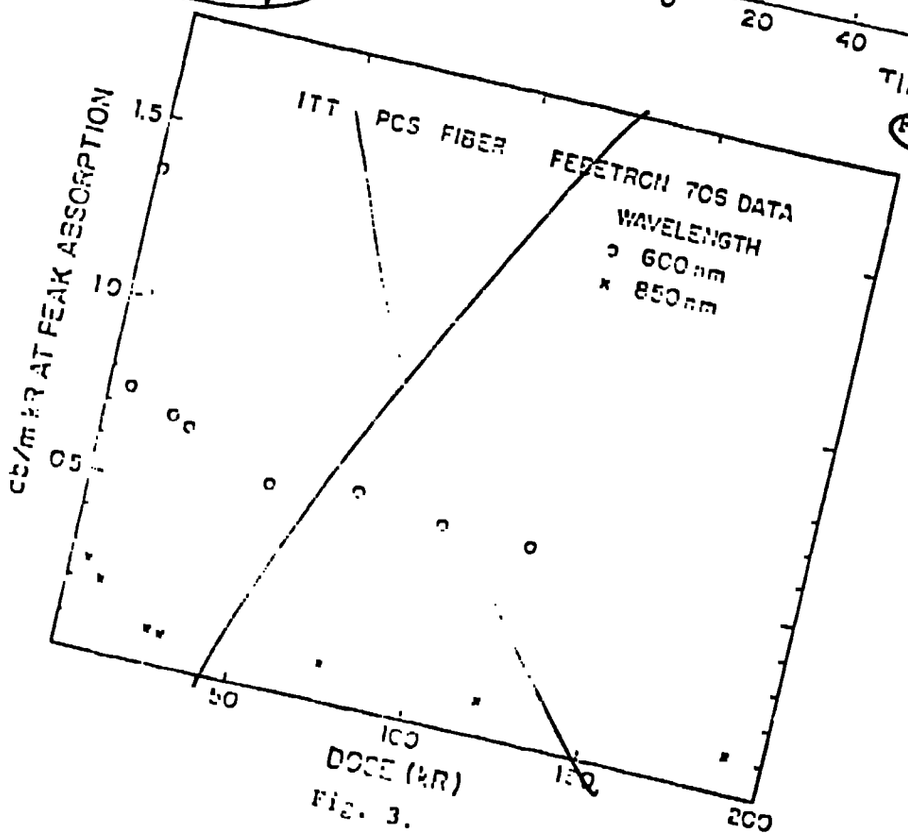

Fig. 3.

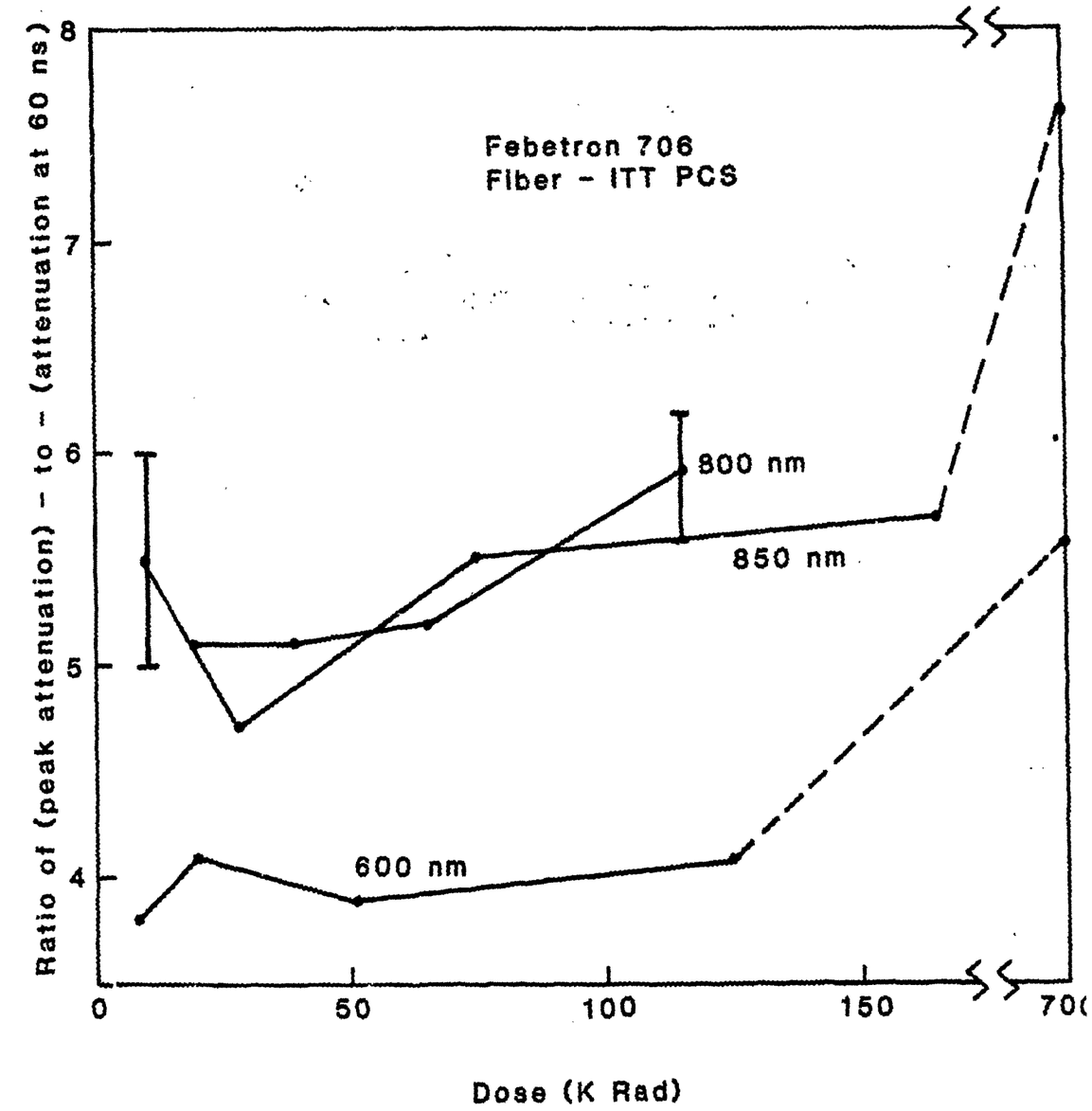
Ratio of (peak attenuation) - to - (attenuation at 60 n
8
7
6
5
4
Febetron 706
Fiber - ITT PCS
800 nm
850 nm
600 nm
0
50
100
150
70
Dose (K Rad)

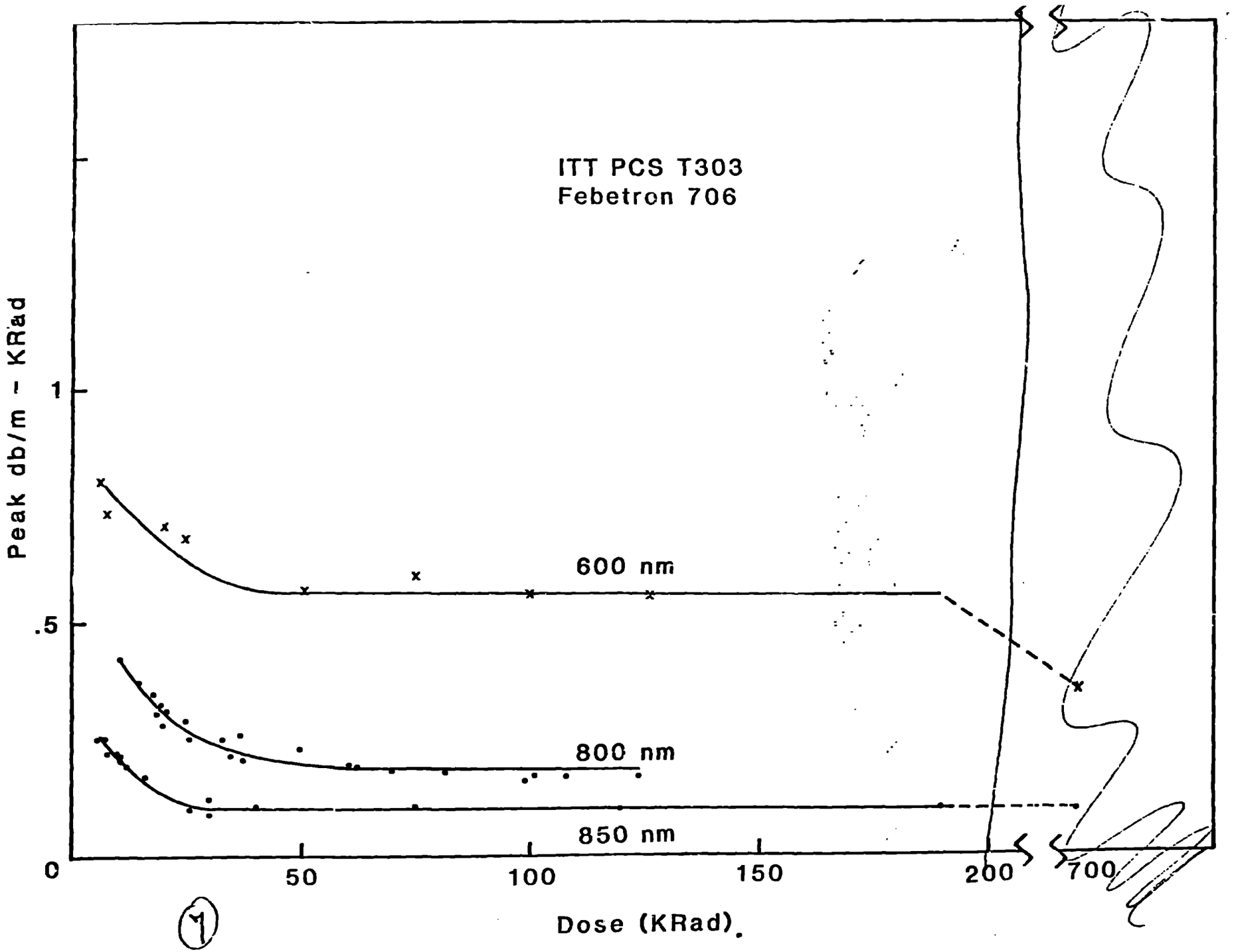
ITT PCS T303
Febetron 706
Peak db/m - KRad
1
.5
0
600 nm
800 nm
850 nm
50
100
150
200
700
Dose (KRad)

(7)

distinguish

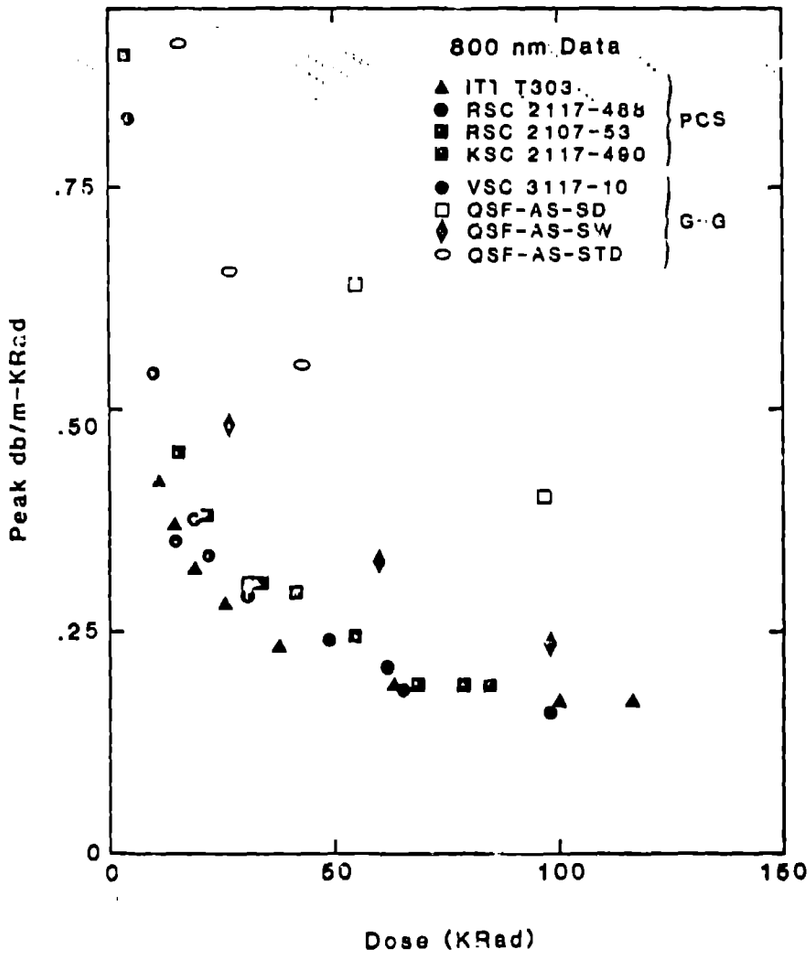

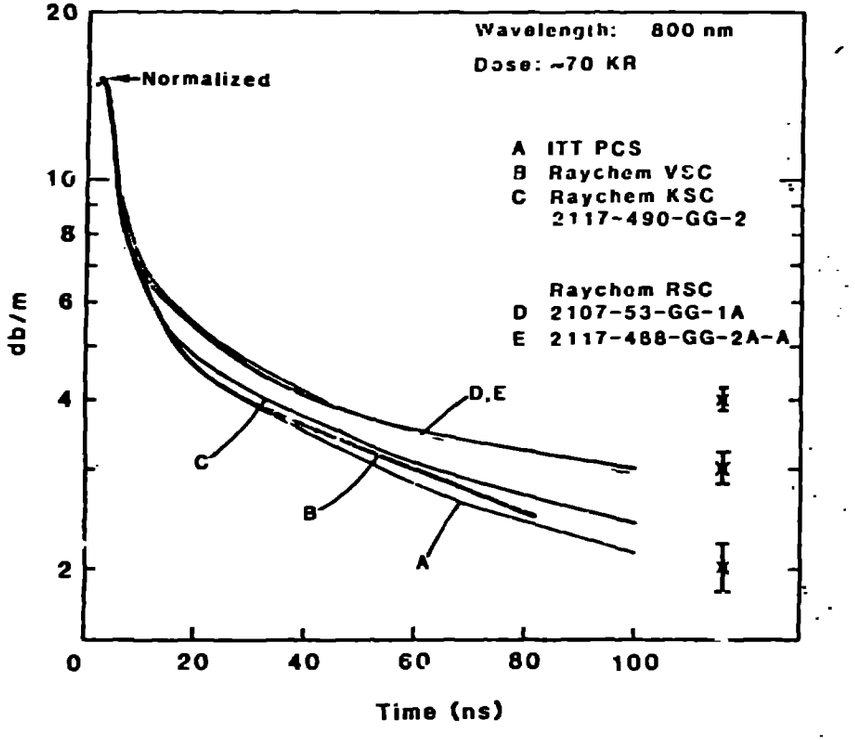
Wavelength: 800 nm
Dose: ~70 KR
Normalized
A ITT PCS
B Raychem VSC
C Raychem KSC
2117-490-GG-2
Raychem RSC
D 2107-53-GG-1A
E 2117-488-GG-2A-A
D,E
C
B
A
db/E
20
10
8
6
4
2
0
20
40
60
80
100
Time (ns)

q

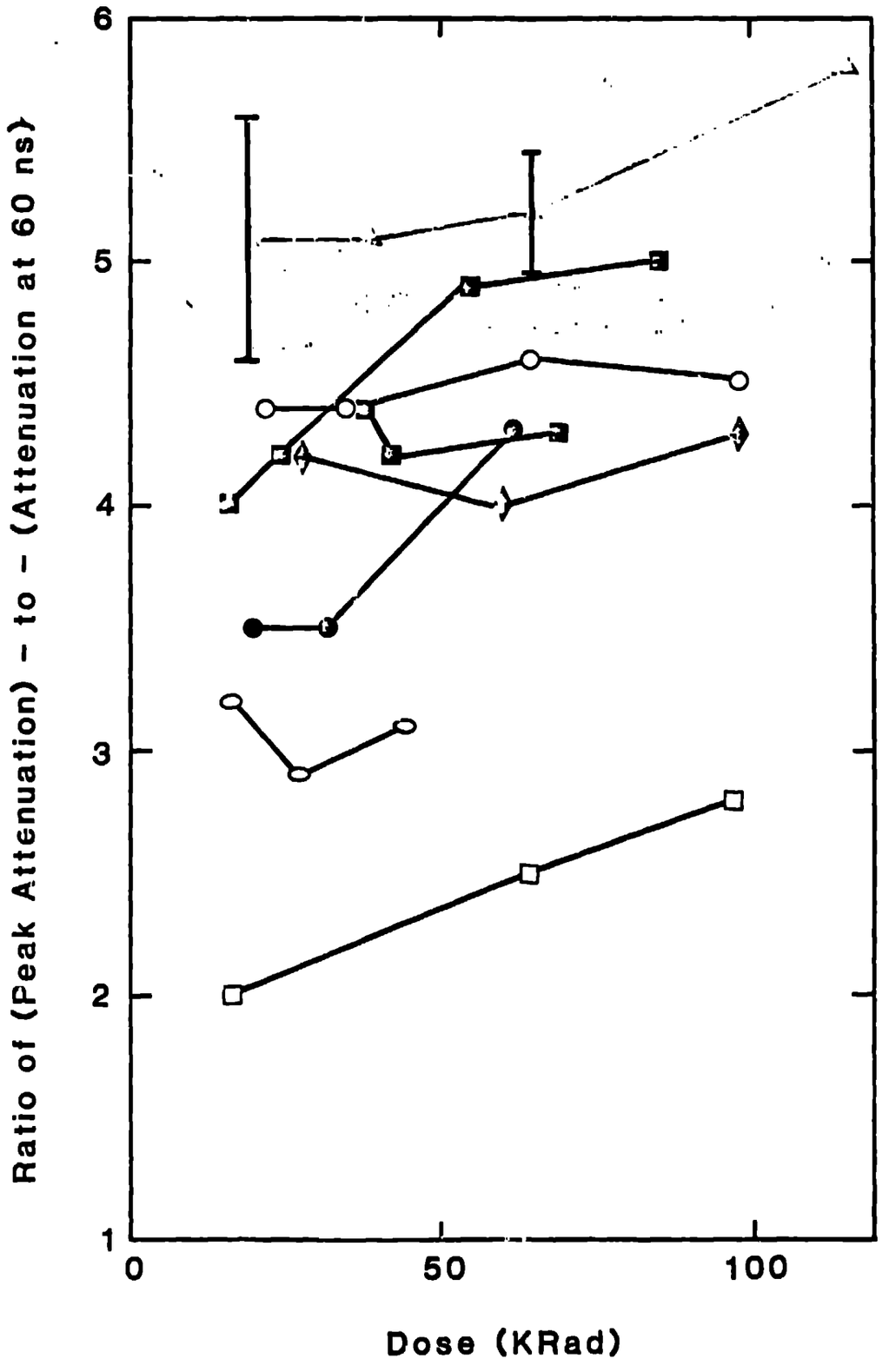
Ratio of (Peak Attenuation) - to - (Attenuation at 60 ns)
6
5
4
3
2
1
0
50
100
Dose (KRad)

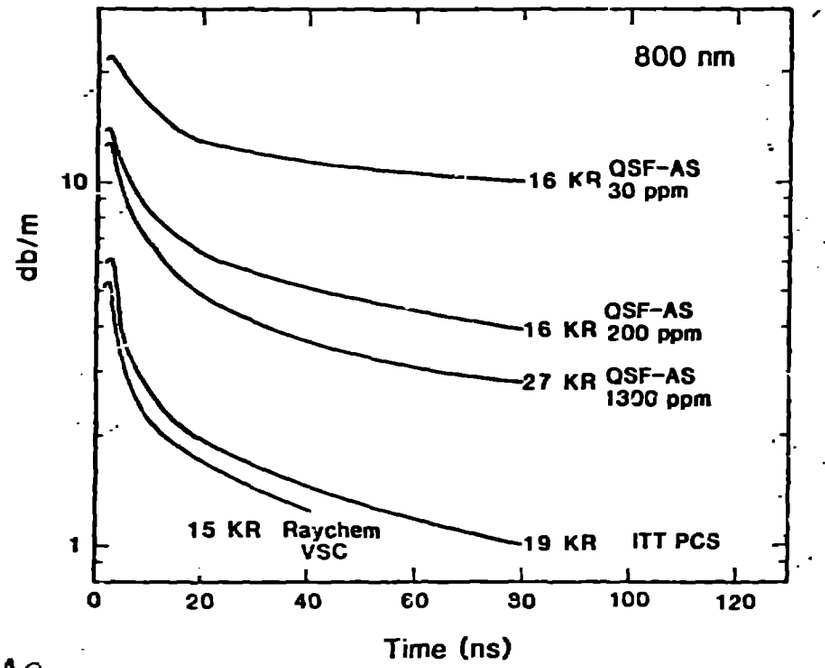

(11)

Typical attenuation measured for the fibers exposed to similar dose rate levels